TUM-HEP 1257/20

A first approach to the study of the QCD phase transition in cosmology

Aldo Gamboa,[1*] **David Guzmán,**[1†] **Víctor Knapp**[1‡]
José Padua[1,2§] **and Saúl Ramos-Sánchez**[2,3¶]

[1] *Facultad de Ciencias, Universidad Nacional Autónoma de México, POB 70-542, Cd.Mx. 04510, México*

[2] *Instituto de Física, Universidad Nacional Autónoma de México, POB 20-364, Cd.Mx. 01000, México*

[3] *Physik Department T75, Technische Universität München, James-Franck-Straße 1, 85748 Garching, Germany*

Abstract

The cosmological QCD confinement is studied as a first order phase transition with the MIT bag model. The basic concepts of cosmology, phase transitions, nucleation theory are introduced. The equations of the dynamics of the transition are established and a program is supplied for the numerical solution. The solution of the dynamics of the transition are studied varying the surface tension of the bubble, the critical temperature and the number of dynamical quarks for current limits. The objective of this article is to introduce the basics of the cosmological QCD phase transition for an advanced undergraduate or graduate student.

[*] aldojavier@ciencias.unam.mx
[†] david_guzmanr@ciencias.unam.mx
[‡] victorknapp@ciencias.unam.mx
[§] jospadua@ciencias.unam.mx
[¶] ramos@fisica.unam.mx

1 Introduction

Aldo David Víctor José Saúl

The model that best fits all observed properties of the Universe at scales as large as a few hundred Megaparsecs[1] is known as ΛCDM model, a shorthand for a description of a highly homogeneous and isotropic space-time, populated by common matter (frequently dubbed *baryonic matter*), as well as Cold Dark Matter (CDM) and dark energy, encoded in a so-called cosmological constant Λ. Although the latter two components have not yet been observed directly in our Universe, there is strong (gravitational) evidence of their existence.

According to the ΛCDM model, most of the observable matter that shapes the Universe as we know it was created during the three minutes that followed the often called *big bang*, the beginning of time about 14 billion years ago. The whole observable Universe, originally confined to a point, experienced a sudden and violent expansion, which led, when the Universe was barely 10^{-32} s old, to the appearance of particles and antiparticles in equal amounts, and light, distributed homogeneously in an already vast space. Since its initial temperature as high as 10^{26} K, due to its homogeneous distribution, the hot content of the Universe can be described as a thermal bath with the properties of a perfect fluid. As the volume of the Universe continued its growth, the pressure and temperature of the hot fluid were smoothly reduced.

About 10^{-10} s after the big bang, when the temperature had reduced to nearly 10^{15} K, it is thought that a series of conditions [1] allowed for a (tiny) imbalance between matter and antimatter that produced the matter domination that rules the Universe today. At the level of elementary particle physics, one of these conditions is that the rates at which matter and antimatter interact must differ, which happens (non-perturbatively) even in the Standard Model (SM) of particle physics [cite to PDG]. Another important condition is that this process must have occurred out of thermal equilibrium, so that it could not be reversed. In an expanding Universe, this naturally happens if the system experiences first order phase transitions, which are indeed likely to be part of the cosmological history. The study of one of these phase transitions of the state of matter in the early Universe is at the core of this work.

At early times, besides gravity, observable matter experienced the electroweak and strong fundamental forces, as described by the SM. While the former is very important for both the generation of mass and the dynamics of light and electrically-charged particles, and could also have been partly responsible for the matter-antimatter asymmetry (see e.g. [cite to EW baryogenesis]), we shall focus here only on the cosmological influence of strong nuclear interactions.

Protons, neutrons and other similar particles, called altogether *hadrons*, are composite particles, i.e. they are built out of more elementary particles called *quarks* and antiquarks:[2] spin-1/2 fermions which carry "color", the fundamental charge of strong interactions[3] and fractional electric charges (either $\pm 2/3$ or $\mp 1/3$). The best description of these colored particles and their strong interactions is provided by a quantum field theory known as *Quantum Chromo-Dynamics* (QCD), in which the exchange among quarks of 8 different spin-1 bosons called *gluons* is the origin of the strong force that, at today's average temperatures, holds protons together in the atomic nuclei (overcoming the electromagnetic repulsion) and binds quarks together within hadrons.

[1] A parsec (denoted as pc) amounts to about 3.26 lightyears or 3.08×10^{13} km.

[2] An antiquark is the antiparticle of a quark; it distinguishes from a quark only due to its opposite physical charges, such as electric and color charge.

[3] This charge can be thought of as somewhat similar to the electric charge, but with three different values, typically named red, green and blue.

Two kinds of hadrons have been observed, *baryons* and *mesons*. Baryons, such as protons and neutrons, consist of three quarks while their antiparticles, antibaryons, consist of three antiquarks. Mesons, as pions and kaons, are made up of one quark and one antiquark. Clearly, due to their structure, mesons do not contribute to an imbalance between matter and antimatter, but baryons do. A way to measure the asymmetry of matter over antimatter is then to observe the difference on the amount of baryons and antibaryons. This can be achieved by considering the so-called *baryon number*, defined by

$$\mathcal{B} = \frac{1}{3}(n_q - n_{\bar{q}})\,, \tag{1}$$

which compares the number of quarks n_q against the number of antiquarks $n_{\bar{q}}$. Clearly, mesons lead to $\mathcal{B} = 0$ and a baryon would be counted as $\mathcal{B} = 1$.

However, hadrons have not always existed. It is known that QCD at higher temperatures or high quark chemical potentials, e.g. at the temperatures of the early Universe (larger than some billion Kelvin), allows for the quarks to be almost free (a remarkable phenomenon known as *asymptotic freedom* [2,3]). The result is a hadron-free hot state of electrically charged matter composed of quarks and gluons, that is known as *quark-gluon plasma* (QGP). Since, despite counting baryons when hadrons are present, $\mathcal{B}$ considers the numbers of quarks and antiquarks, one may expect that $\mathcal{B} \neq 0$ in a given volume of the QGP.

Observations at particle colliders indicate that quarks and gluons confine to build up hadrons at energies roughly around 160 MeV [4] or equivalently at a temperature 1.86×10^{12} K, below which quarks and gluons cannot be observed individually. According to the standard cosmological model, the Universe achieved that temperature when it was only about 10^{-5} s of age. Quarks and gluons contained in observable hadrons are said to be in a hadronic state. The transformation of quarks and gluons in the QGP to the hadronic state, and vice versa, is the QCD phase transition or *confinement-deconfinement transition*. This paper is devoted precisely to the study of the dynamics of matter during this phase transition.

If the QCD phase transition is first order (as certain scenarios suggest, see e.g. [5, 6]), then, according to nucleation theory, it must have occured through the formation of *bubbles* of hadronic matter in the QGP, with their subsequent growth until they populated the whole Universe. The internal regions close to the surface of the bubbles would concentrate a dense baryon number $\mathcal{B}$ due to the difficulty for the hadrons to diffuse [7], giving a net accumulation of baryons at the end of the transition. The slow diffusion of hadrons arises from the electromagnetic interaction between charged baryons (like protons) and the electron-positron background present inside the bubble [8]. Since most of the internal region of the bubbles does not contain baryons, the baryon density (i.e. the baryon number per unit volume) in the QGP is higher than in the hadronic phase, giving an inhomogeneity known as *baryon density contrast*.

Historically, one of the main interests in a first order QCD phase transition was the possibility to influence Big Bang Nucleosynthesis[4], since this kind of phase transitions allows the existence of regions with inhomogeneities which may have had an impact in the formation of the first elements. Nevertheless, the minimal requirement for this scenario is that the mean bubble nucleation distance has to be greater than the proton diffusion length ($\sim$ 3 m at the time of the QCD phase transition) [9]. As it will be seen in (where? in section...), the required value for the mean distance between inhomogeneities is achieved only under certain conditions.

[4]Big Bang Nucleosynthesis is the process in which the nuclei of the lightest elements (^{4}He, D, ^{3}He and ^{7}Li) were produced in the early Universe (from 10 s to 20 min in the range of temperatures from 10^{10} K to 10^9 K). This process is one of the main observational evidences for the ΛCDM model.

Recently, the interest in a possible QCD first-order phase transition has been reborn due to the discovery of gravitational waves [10]. Cosmological first-order phase transitions could have produced gravitational waves due to the collisions of the bubbles made during the transition. The generated power spectrum could depend on the bubble radius and on the time that the transition lasted [11].

Although current knowledge of cosmology indicates that the most probable scenario is that the QCD phase transition was a crossover [12], we think that the study of a first order QCD phase transition may give a student insight into modern cosmology research and will provide tools to understand more realistic scenarios. Furthermore, it will enforce concepts that may be already known to the student but had not been applied in a cosmological context, such as the thermodynamics of a phase transition. Aside from this, some people actually do propose that, due to our current ignorance of the early history of the Universe, a QCD first order phase transition could have happened. For example, according to [13], if three or more dynamical quarks[5] were present during the QCD phase transition, a first order phase transition would have happened producing black holes already detected by LIGO/VIRGO detectors. Discussions on other scenarios where a QCD first order phase transition is realized can be found in [14] and [15].

This paper is organized as follows. In section 2, we present some basic notions of cosmology needed to understand the basic setup of our work; in section 3, we discuss the phenomena of phase transitions emphasizing first order phase transitions, and then, in section 4, we relate this discussion to the QCD phase transition and we talk about the collective properties of the QGP plasma and the hadron gas. In section 5, we review some aspects of nucleation theory necessary to compute the nucleation rate of bubbles for the QCD phase transition scenario and we present the most important parameters needed to understand the general behavior of the generated bubbles. In section 6, we present the theoretical framework used to describe the growth and expansion of the nucleated bubbles in a radiation-dominated flat Universe, arriving to a system of integro-differential equations. In section 7, we present and discuss the results obtained for the evolution of the bubbles during the QCD phase transition, and finally, in section 8 we give the conclusions and suggestions for future work. To simplify somewaht our notation, in this paper use natural units, i.e. we set $c = k_B = \hbar = 1$.

2 Some Standard Cosmology Basics

Modern cosmology studies the properties of the universe as a whole at scales of the order of few$\times$100 Mpc, with the aim of understanding its origin, evolution and dynamics. Some of the fundamental questions that cosmology addresses include the origin of the large-scale structure observed in the Universe, the reason of the evident predominance of matter over antimatter and the origin of the lightest chemical elements.

The ΛCDM model is based on two main premises: i) the *cosmological principle*, which states that the Universe is homogeneous and isotropic, and ii) the assumption that the physics laws that we know today were (and will remain) valid at all times. One of such laws is the theory of general relativity, which is known to be the most appropriate description of gravitational interactions in terms of the interplay between the geometry of space-time and its content. If general relativity has always held, it can describe the dynamics of our Universe, provided one knows at some level its geometry and content.

[5] A dynamical quark have a mass much smaller than the energy scale of the system, given in this case by the temperature.

In general relativity, the geometry of space-time with three spatial dimensions and a time is determined by the components of a metric tensor, $g_{\mu\nu}$ with $\mu, \nu = 0, \ldots, 3$, which can be roughly understood as the set of rules that teach us how to measure the separation between events occurring at different positions and times. Within the formalism of (pseudo-)Riemannian geometry, the metric tensor allows one to characterize how curved the shape of a space-time is in terms of the components of the Riemann tensor, $R^{\alpha}{}_{\mu\beta\nu}$, the Ricci tensor, $R_{\mu\nu}$, and the Ricci scalar, R. If all these quantities vanish in a space-time (for all index combinations), it is flat; otherwise, it has a non-trivial curvature. General relativity relates the curvature with the dynamics of its contents by the so-called Einstein's field equations (in units such that $c = 1$)

$$R_{\mu\nu} - \frac{1}{2} R\, g_{\mu\nu} = 8\pi G\, T_{\mu\nu}\,, \qquad \mu, \nu = 0, \ldots, 3\,, \tag{2}$$

where G is the Newtonian gravitational constant and $T_{\mu\nu}$ are the components of the energy-momentum tensor that describes the flux and density of the energy and momentum of the contents of the space-time. Note that $T_{\mu\nu} = 0$, for all $\mu, \nu = 0, \ldots, 3$, is always satisfied in a flat space-time. Eqs. (2) indicate that the dynamics of particles in a space-time are governed by its geometry, and, conversely, that the geometry is influenced by its contents.[6] Since the conception of general relativity, it was clear that this surprising statement can be applied to describe our cosmology.

It can be proven that the cosmological principle is satisfied by the space-time described by the Friedmann-Lemaître-Robertson-Walker (FLRW) metric $g_{\mu\nu}$, associated with the space-time interval (we use Einstein's convention of implicit summation over repeated indices)

$$ds^2 = g_{\mu\nu}\, dx^\mu dx^\nu = dt^2 - a(t)^2 \left(\frac{dr^2}{1 - k\, r^2} + r^2\, d\vartheta^2 + r^2 \sin^2 \vartheta\, d\varphi^2 \right)\,, \tag{3}$$

where $x^0 = t$ is the *cosmic time*, $x^1 = r$, $x^2 = \vartheta$ and $x^3 = \varphi$ are the usual spherical coordinates, and $a(t)$ is called cosmic *scale factor*. The scale factor is a time-dependent measure of the relative expansion of the Universe with respect to its value at present time t_0, conventionally defined to be $a(t_0) = 1$. One can assume that $a(t = 0) = 0$ at the beginning of cosmic time.

The coordinates x^μ are known as *comoving coordinates* and do not change with the expansion of the Universe. In a *comoving frame* the matter of the Universe which only moves with the expansion, is at rest, so that one can define a *comoving volume* which remains constant with the expansion. In this volume, the number densities of objects in rest with respect to the comoving frame, remain constant.

The parameter k in eq. (3) is a constant that contains the scalar information about the curvature (see appendix A) of the three-dimensional space (not the whole space-time). $k = 0$ corresponds to a spatially-flat universe (Euclidean space), while $k = 1$ describes a positively curved universe (elliptical space), and $k = -1$ a negatively curved universe (hyperbolic space). It is important to stress that the full space-time described by the FLRW metric has non-vanishing curvature for any value of k.

Once the geometry of a cosmologically consistent space-time has been specified, we can focus on the properties of the cosmic content. First, note that an ideal gas is homogeneous and isotropic. Thus, demanding that the Universe satisfies the cosmological principle amounts to requiring that the pressure $P(t)$ and energy density $\epsilon(t)$ of the contents of the Universe be described by the energy-momentum tensor of an ideal gas [18]. It is known that the components

[6] Since this work does not pretend to be a pedagogical essay on general relativity, we refer the interested to accessible textbooks, such as [16, 17].

of such an energy-momentum tensor are represented by the matrix

$$(T^{\mu}{}_{\nu}) = \begin{pmatrix} \epsilon(t) & & & 0 \\ & -P(t) & & \\ & & -P(t) & \\ 0 & & & -P(t) \end{pmatrix}, \tag{4}$$

where $\epsilon(t)$ and $P(t)$ can describe several *species* or thermally distinguishable types of content. Different species satisfy different thermodynamic equations of state. If the interactions among species are negligible and, in particular, do not allow for conversions of one species into another, then the energy density and pressure decompose as $\epsilon(t) = \sum_i \epsilon_i(t)$ and $P(t) = \sum_i P_i(t)$, respectively, where the index i labels the species.

Given the geometry described by the interval (3) and the energy-momentum tensor (4), the dynamics of the Universe is established by the equations of general relativity (2), which are equivalent to the *Friedmann equations*:

$$H^2 + \frac{k}{a^2} = \frac{8\pi G}{3}\epsilon\,, \tag{5a}$$

$$\frac{\ddot{a}}{a} = -\frac{4\pi G}{3}\left(\epsilon + 3P\right), \tag{5b}$$

where $H(t) \equiv \dot{a}/a$ is known as the *Hubble parameter* at some time. In terms of the so-called *critical density*, $\epsilon_c(t) \equiv 3H^2/8\pi G$, we can rewrite eq. (5a) as

$$\frac{k}{a^2H^2} = \frac{8\pi G}{3H^2}\epsilon - 1 \equiv \frac{\epsilon}{\epsilon_c} - 1, \tag{6}$$

and see that $k = 0$ is satisfied only if $\epsilon = \epsilon_c$ at time t. This reveals that ϵ_c corresponds to the energy density of the Universe when the space is flat. At present time, $t = t_0$, independent measurements of the Hubble parameter $H_0 \equiv H(t_0)$ and the energy density of the Universe ϵ_0 suggest, in this context, that $k = 0$, i.e. the three dimensions of our Universe build today a flat space [19]. The origin of this flatness is typically attributed to the existence of a very short period of exponential expansion known as *cosmological inflation* that occurred less than 10^{-32} s after the beginning of time. Although the details of inflation are an open question, we can safely assume that $k = 0$ has been valid especially during the formation of hadronic matter, which is the epoch that interests us.

Replacing eq. (5b) and the time-derivative of eq. (5a) in $\dot{H} = -H^2 + \ddot{a}/a$, we find the general relation[7]

$$\frac{d\epsilon}{dt} = -3H(\epsilon + P) = -3\,\frac{1}{a}\frac{da}{dt}(\epsilon + P), \tag{7}$$

which allows one to establish the cosmological dynamics of ϵ and P.

Since only two of the three eqs. (5) and (7) are independent, to find the solutions of a, ϵ and P, we use additionally the equation of state of the contents of the Universe, which we specify for each species as

$$P_i(t) = w_i\,\epsilon_i(t), \tag{8}$$

where w_i is assumed to be a constant value in time. As a good approximation, we can split all forms of contents of the Universe in three species: relativistic particles with $w_i = 1/3$, non-relativistic particles with $w_i = 0$, and dark energy with $w_i = -1$ (negative presure), responsible for the accelerated expansion of the Universe observed today.

[7]This equation can be obtained also by demanding energy-momentum conservation in a dynamic space-time, which formally is stated by the continuity equation $T^{\mu\nu}{}_{;\nu} = 0$.

Even though all species have coexisted at all times, at each epoch the Universe dynamics has been dominated by a different species, that is, the energy density has been mostly determined by one species. In the ΛCDM model, after inflation, the Universe is supposed to have been dominated by relativistic particles, which are broadly also called "radiation", even though all sorts of relativistic matter (not only photons) are included. After the formation of the first nuclei, when the Universe was around $10,000$ years old and had cooled down so that only light and neutrinos moved at relativistic speeds, the Universe was dominated by non-relativistic clumping matter. And finally, when the Universe was about 8×10^9 years old, it is thought that a form of dark energy started its domination on the cosmological evolution. As we shall shortly see, these changes are due to the form of the solutions for ϵ.

We can easily solve eq. (7) when one species dominates the Universe, which implies that, instead of eq. (8), we can use $P = w\,\epsilon$ with $w = 1/3, 0, -1$. As functions of the scale factor, we find

$$\epsilon(a) \propto \begin{cases} a^{-4} & \text{relativistic particles } (w = 1/3)\,, \\ a^{-3} & \text{non-relativistic particles } (w = 0)\,, \\ \text{const.} & \text{dark energy } (w = -1)\,. \end{cases} \tag{9}$$

Using this result in eq. (5a), we observe that the rate at which the Universe expands depends on its contents, according to

$$a(t) \propto \begin{cases} t^{1/2} & \text{relativistic particles } (w = 1/3)\,, \\ t^{2/3} & \text{non-relativistic particles } (w = 0)\,, \\ e^{H_0 t} & \text{dark energy } (w = -1)\,. \end{cases} \tag{10}$$

Since $a(t)$ grows in all cases, it is clear from eq. (9) that the energy density of "radiation" reduces faster than the energy density of non-relativistic particles while it does not change for dark energy, explaining why ϵ can be dominated by different species at different times.

During the QCD phase transition, both the QGP and the hadrons are relativistic. Thus, as we shall see, it is important to know how the energy density varies as a function of the temperature of the collection of particles during the "radiation"-dominated epoch. With this purpose, we apply now some results from statistical mechanics. It is known that the energy density is given by [20, p.43]

$$\epsilon = \frac{g}{(2\pi)^3} \int d^3p\, f(p) E(p), \tag{11}$$

where g denotes the number of degrees of freedom of the particles in the system,[8] p is their momentum and $f(p)$ is known as the particle distribution function, which denotes the average number of particles in a state with energy $E(p)$. Note that for relativistic particles with mass $m \ll p$, the energy is given by $E(p) = \sqrt{p^2 + m^2} \approx p$. For an ensemble of fermionic (half-integer spin) or bosonic (integer spin) particles, the distribution function takes the form [20, p.43]

$$f(p) = \frac{1}{e^{\frac{E(p)-\mu}{T}} \pm 1}\,, \tag{12}$$

where μ is the total chemical potential and T is the temperature of the system. The positive sign corresponds to the so-called Fermi-Dirac distribution (describing fermions) and the negative sign yields the Bose-Einstein distribution (for bosons).

[8] This counts the degeneracy of the system, i.e. the total number of values that accept the independent quantum numbers (such as spin, color, etc.) of all different particles (e.g. photons, electrons, quarks, etc.) intervening in the dynamics of the system.

A chemical potential μ_i is always associated with a conserved particle number N_i (this conserved quantity has a definition similar to (1), which takes into account the difference between the number of particles and antiparticles; note that in this notation $N_{\mathcal{B}} = \mathcal{B}$) and encodes the released or absorbed energy of the system when the number of particles of species i in the system changes. In this case, the chemical potential μ is the sum of all the chemical potentials μ_i related to all the relativistic conserved particle numbers N_i. It is known that at the temperatures at which the transition from the QGP to a hadronic gas took place or higher, all the relativistic conserved particle numbers satisfied $N_i \approx 0$. This is a consequence of the smallness of the measured baryon-to-photon ratio, $\eta = \mathcal{B}/N_\gamma \sim 10^{-10}$, where $\mathcal{B}$ and n_γ are the baryon number (1) and the photon number, respectively, which implies that total chemical potential is negligible[9]. Thus, considering $\mu \ll T$, eq. (11) yields

$$\epsilon(T) = \frac{\pi^2}{30}\, g\, T^4 \times \begin{cases} 1 & \text{for bosons}\,, \\ \frac{7}{8} & \text{for fermions}\,, \end{cases} \tag{13}$$

which establishes the explicit relation between the energy density for relativistic particles and the temperature. Furthermore, comparing eqs. (9) and (13) for relativistic particles, we find that $T \propto a^{-1}$. As anticipated, the temperature decreases as the Universe expands.

3 Phase transitions and thermodynamics

In order to understand the conversion from (almost) free quarks and gluons in the QGP to confined hadrons, let us first study some generalities of phase transitions.

Boiling water or making ice are typical examples of drastic changes of the thermodynamic properties of water. Liquid water, ice and steam are three distinct states of water known as *phases*. The phases of water exhibit important physical differences even if their (molecular) constituents are the same. In order to change from one phase to another, water has to experience a physical process associated with the change of one of his thermodynamic variables (e.g. increasing or decreasing its temperature). There is more than one way for water (and any other thermodynamic system) to change phase.

The special type of phase change that water undergoes when it is boiled or frozen is known as *phase transition*. In a phase transition, the drastic change of its properties can be formally understood from a non-analyticity (divergences or discontinuities in the derivatives) in the free energy of the system. Phase transitions can be classified into: *first order phase transitions* with the presence of *latent heat*[10] and *second order phase transitions* with no latent heat [21].

Es necesario hablar de U? All the thermodynamic quantities of a system are encoded in the internal energy $U(S, V, N_i)$, that depends on the entropy S, the volume V and the number N_i of particles of type i, which are all extensive properties. The extensive variables, like the volume, entropy and particle number; of the system can be obtained by extremizing $U(S, V, N_i)$ while the intensive variables, like the temperature, pressure and chemical potential; are the partial derivatives of $U(S, V, N_i)$. From a physical perspective, U can be interpreted as the work required to *create* the system. Sometimes there is a constraint on our system, in which case it is convenient to use U's Legendre transformations, also known as thermodynamic potentials. For example, if the system is in contact with a *heat reservoir* (so the temperature is fixed),

[9] The chemical potential of a particle is minus the chemical potential of an antiparticle. So, the conserved number of particles N_i is an odd function of the different chemical potentials μ_i.Thus, if $N_i \sim 0$ for all i, then $\mu_i \approx 0$ for all i [18, p.531].

[10] Amount of heat released or supplied during the phase transition.

it is useful to use the Helmholtz free energy $F(T, V, N_i) := U - TS$ instead of U. Now the values taken by V and N_i are those that extremize F at a given T. In this case F is to be interpreted as the work required to create the system on an environment of temperature T. Landau developed a formalism to study phase transitions where the free energy also depends on a new variable called the *order parameter* $\mathcal{O}$, so that $F = F(T, V, N_i; \mathcal{O})$. The order parameter is a quantity that changes according to the phase the system is in. It is generally chosen so that it is zero during a phase and different from zero in the other phase. For example, in the liquid-gas phase transition the order parameter is the difference of densities $\mathcal{O} = \rho - \rho_{gas}$. An extra equilibrium condition is then added in order to extremize F, namely: $\frac{\partial F}{\partial \mathcal{O}} \stackrel{!}{=} 0$. The solutions to this equation correspond to different phases and their respective Helmoltz free energies F_* are obtained by the evaluations $F(T, V, N_i, \mathcal{O}_*)$ with the corresponding $\mathcal{O}_*$. Qué es $\mathcal{O}_*$?

Furthermore, the change in the order parameter is different depending on the type of phase transition. Physically, the existence of a latent heat implies that while this heat is being supplied or released during the phase transition the system is in a mixture of the two phases. Therefore, in a first order phase transition the order parameter suffers a discontinuous jump. For example, when boiling water from a liquid phase, the order parameter starts with an order parameter $o \neq 0$ at the beginning of the phase transition but when the transition ends and all the water is now vapor, then $o = 0$. For a second order phase transition the order parameter changes continuously.

The latent heat L can always be written as

$$L = T\Delta S = V\Delta\omega, \tag{14}$$

where ΔS is the change of the entropy from one phase to another, V is the volume and $\Delta\omega$ is the change in the entalphy density $\omega = \epsilon + p$. From equation (14), we can see that the non-analiticity in the free energy is reflected in the first derivative of the free energy which is the entropy $S = \frac{\partial F}{\partial T}$.

Another type of changes in matter are the so called *crossovers*. In Figure 1(a), we show a schematic of the phase diagram of the liquid-gas phase transition of water. The dot is called the critical point (CP). The transition from liquid to gas happens as a first order phase transition along the transition line which is the continuous line in the Figure 1(a). In the CP, the phase transition is of second order. For temperatures higher than the critical temperature T_c and pressures higher than P_c there is not a real phase transition because the non-analiticities in the free energy vanish. Thus, water in these conditions is neither liquid nor gas but a different state of matter that effuses through solids like a gas and dissolves like liquid [22]. Nevertheless, there is a continuation to the transition line called the *Widom line* which is depicted as the dotted line in Figure 1(a). Crossing the Widom lines is known as a crossover transition. In Ref. [23] it was shown that, when crossing the Widom line, argon fluid presented a drastic change in sound dispersion[11]. Thus, the behaviour of the fluid changed drastically when crossing the Widom line although it is not a real phase transition.

In Figure 1(b) it is presented the heat capacity, depicted as the continuous red line, and the density, depicted as the dotted black line, during a isobaric first order liquid-gas phase transition in oxygen at constant pressure of 4 MPa and the same curves for a crossover through the Widom line at 10 MPa. In the 4 MPa there is the expected divergence in the heat capacity that happens during a first order liquid-gas phase transition with the corresponding discontinuous jump in the density which is the order parameter. For the crossover transition the heat

[11] The change in speed of an acoustic wave depending on its wavelength

capacity exhibits a maximum instead of a divergence and, at nearly the same temperature, the density has an inflection point which corresponds to a maximum in the derivative of the density with respect to the temperature. The (pseudo)critical temperature of the crossover is then defined at either the inflection point in the order parameter or at the maximum of the heat capacity. At temperatures and pressures nearly above the CP, these two pseudo-critical temperatures coincide as in [24], but as the temperature and pressure increases the two pseudo-critical temperatures start to separate from each other [25]. Furthermore, an uncertainty can be related to the curvature of the derivative of the order parameter or of the heat capacity, with the uncertainty vanishing as the curvature goes to infinity (which corresponds to the case of a real first order phase transition). This uncertainty represents the fact that a crossover does not happen sharply as a real phase transition at a unique temperature but occurs continously across the range of temperatures given by the interval of the uncertainty. Thus, the Widom line is actually a *Widom band*, which separates into two bands corresponding for the two possible pseudocritical temperatures.

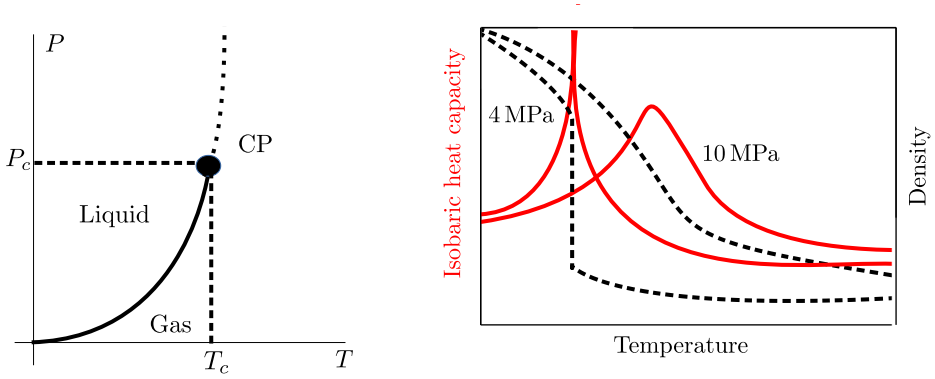

Figure 1: (a) Phase diagram of water: the continuous line represents the first order phase transition coexistence line. The big dot is the critical point (CP) at which water exhibits a second order phase transition. The dotted line is the Widom line corresponding to the crossover transition [26]. (b) An isobaric liquid-gas phase transition in oxygen: the density, depicted as the dotted black line, and the heat capacity, depicted as the continuous red line, as a function of the temperature during a first order phase transition at constant pressure $P = 4\,\text{MPa}$, and during a crossover transition at constant 10 MPa. Figure based on Ref. [24] with data from [27].

4 The QCD Phase Transitions

According to our discussion in the Introduction, the quarks that made up baryons and mesons can become free particles at high temperatures or high chemical potentials. This process is known as *deconfinement* and it corresponds to a phase transition. The confinement phase transition can be analyzed through an order parameter as was mentioned in Section 3. Currently, very large computer programs are made to simulate QCD in what is known as *Lattice QCD* (LQCD). The objective is to find when and how the parameter order changes to establish the character of the confinement QCD phase transition. In order to give more insight about the character of the confinement phase transition, we need to introduce another QCD phase transition known as the *chiral phase transition*[12], which is associated with the mass change

[12]Although the chiral phase transition will only be slightly discussed in this text because is not our main concern, in modern QCD research it is of huge interest. For more information about the spontaneous chiral

in the quarks. When quarks are confined in hadrons, it is said that the hadrons are formed by *constituent quarks* which have the same physical properties as the quarks in the QGP, but have a higher mass (the up quark in the QGP has a mass of ~ 2 MeV, whereas the constituent up quark in a proton has a mass of ~ 300 MeV).

The phase diagram of both (chiral and confinement) phase transitions at finite T and $\mu_{\mathcal{B}} = 0$ as a function of the quark masses is schematically shown in Figure 2, this plot is known as the *Columbia plot* [5,6]. The character of the transition is shown as a function of the light quarks (quark up and quark down), assuming they have the same mass, and of the strange quark mass. For zero quark masses the so-called *chiral limit*, marked by a red point in the lower left corner, is achieved (it is called the chiral limit because in this limit QCD presents chiral symmetry) and the chiral phase transition happens as a first order phase transition. Actually, the chiral transition happens as a first order phase transition for a region near the chiral point marked by the red area in the Figure 2. The dashed line represents the points where the chiral transition is a second order phase transition. For bigger masses, the chiral transition is a crossover. On the other hand, for infinite quark masses the so-called *pure gauge limit*, marked by a blue point in the upper right corner, is achieved (it is called pure gauge limit because in this limit the quarks are so heavy that they are isolated and the only dynamical particles are the gauge particles: the gluons) and the confinement transition is realized as a first order phase transition. Moreover, the confinement transition also happens as first order phase transition for finite masses in the blue area of the Figure 2. The dotted line represents the points where the confinement transition is realized as a second order phase transition. For smaller masses than the dotted line, the confinement is a crossover. According to the current values of the quark masses, the physical point corresponds to a crossover both in the confinement and chiral transition, as indicated by a star in Figure 2.

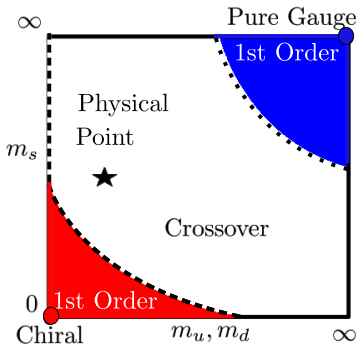

Figure 2: Schematic plot of the character of the confinement and chiral transitions at $\mu_{\mathcal{B}} = 0$ obtained through LQCD as a function of the quark masses [5,6]. This plot is known as the *Columbia Plot*. The chiral transition happens as a first order phase transition in the red area (which includes the chiral limit point (0,0)); as a second order phase transition in the dotted line; and for masses bigger than this line it is a crossover. The confinement transition happens as a first order transition in the blue area (which includes pure gauge limit point (∞,∞)); as a second order phase transition in the dotted line; and for smaller masses than this line it is a crossover. The physical point for the physical quark masses is denoted with a star, where both transitions are crossovers.

Both transitions occur at nearly the same range of temperatures reported in the literature which goes from $150 - 200$ MeV [29, 30]. Unfortunately, for large $\mu_{\mathcal{B}}$ LQCD fails to give a critical or pseudocritical temperature.

symmetry breaking which gives rise to the phase transition see [28].

Several studies have predicted that for a large baryon chemical potential $\mu_{\mathcal{B}} \sim 1$ GeV with $\mu_{\mathcal{B}} = 3\mu_q$[13], where μ_q is the quark chemical potential, then both transitions (confinement and chiral) could be first order [31]. The point where the transition line changes from being a crossover to a first order is called the *critical end point* (CEP). It is generally assumed that the transition lines for the confinement and the chiral phase transitions are the same at least up to the CEP.

Other transitions are present in the QCD Phase Diagram. For example, the liquid-gas phase transition at low temperatures which is typically a first order phase transition but ends up being a second-order phase transition in the last point of the transition line. Another more exotic quark state of matter has been conjectured named as color superconductivity where quarks join to form Cooper-like pairs through a phase transition [29]. The last paragraphs are summarized in Figure 3.

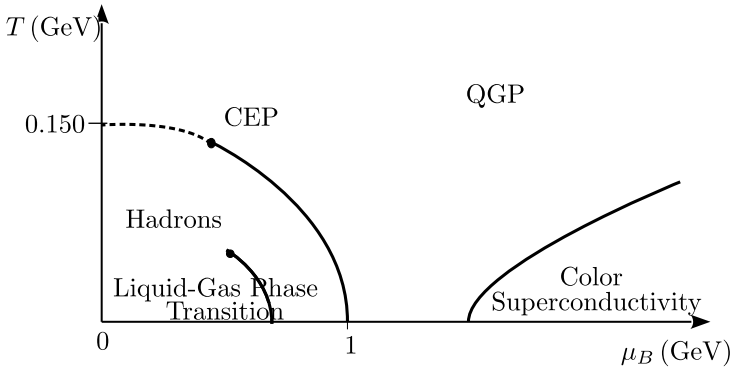

Figure 3: The conjectured QCD ($T - \mu_{\mathcal{B}}$) phase diagram for 2 dynamical quarks and a heavy quark. The dotted line denotes the pseudocritical temperature for the crossover in the confinement transition. The point where the transition changes from a crossover to a first order is called the critical end point (CEP). The solid line after the CEP is the first-order transition line for the confinement. It is also shown the first-order phase transition line for the liquid-gas nuclear phase transition which ends in a second order-phase transition. At the right side of the diagram it is shown the transition line that separates the color-superconductor phase. Image adapted from Ref. [32].

As seen in Figure 3, for $\mu_{\mathcal{B}} \sim 0$ the confinement transition is most likely a crossover. Due to the measured value of the baryon to photon ratio $\eta \sim 10^{-10}$ we know that in the early Universe the chemical potential was about $\mu_{\mathcal{B}} \approx 0$. Thus, according to the observed quark masses, Figures 2 and 3 dictate that the transition must be a crossover. To our current knowledge, this is the most possible scenario. Nevertheless, we think that the study of a QCD first order phase transition can give further insight into cosmology for a student who is beginning to study these topics.

Although not the mayority, some escenarios suggest a possible chiral or confinement first order phase transition. For example, not only three massless quarks could generate a first order chiral phase transition, but also for $N_f \geq 3$ [33]. This could have happened, for example, if the mass of the quarks was suppressed by some mechanism as in [13] leading to an increment of the dynamical quarks. There could also have been a very early confinement first order phase transition, if by some mechanism the baryonic chemical potential satisfied that $\mu_{\mathcal{B}} \sim T$, as stated in [15]. Furthermore, another possibility stated in [14] says that a very early confinement first order phase transition could have been possible if the coupling constant of QCD is modified. In this work, we are going to stay with the assumption that $\mu_{\mathcal{B}} = 0$, $N_f \geq 3$ and that the

[13]This relation comes from the fact that a baryon is made of three quarks.

confinement phase transition is first order.

In order to get the evolution of a cosmological QCD phase transition we need to know the densities and pressures of the confined and deconfined phases. Let us consider the QGP and the hadron gas as ideal relativistic fluids, so that $P = \frac{1}{3}\epsilon$. Then, according to eq. (13)

$$\epsilon = \frac{\pi^2}{30}T^4 \times \begin{cases} g_{QGP}, & \text{QGP .} \\ g_h, & \text{hadron gas.} \end{cases} \quad \text{and} \quad P = \frac{\pi^2}{90}T^4 \times \begin{cases} g_{QGP}, & \text{QGP.} \\ g_h, & \text{hadron gas.} \end{cases}, \tag{15}$$

where $g_{QGP} = \frac{7}{8}g_{QGP,f} + g_{QGP,b}$ and $g_{QGP,f}$ are the fermionic degrees of freedom for the QGP, and $g_{QGP,b}$ the bosonic degrees of freedom for the QGP. Similarly g_h for the hadron gas phase. Let us determine both g's.

The types of particles present in each phase is determined by the corresponding energy. In the range of the estimated critical or pseudo-critical temperatures for the phase transition, there are photons, neutrinos, electrons and muons in both phases (the critical temperature will be discussed in Section 5 but it will be at most of $T_c = 200\,\text{MeV}$). So both phases share the following degrees of freedom:

$$g_{both} = \frac{7}{8}\left(\underbrace{6}_{neutrinos} + \underbrace{4}_{electrons} + \underbrace{4}_{muons}\right) + \underbrace{2}_{photons} = 14.25, \tag{16}$$

where we have used the fact that there are only three left-handed neutrinos in the standard model (according to current limits [34]) and that they have two spin states (so $3 \times 2 = 6$)[14], we have counted the two spin states and the particle/antiparticle possibilities of electrons and muons (so $2 \times 2 = 4$), and we added the two possible polarizations of photons.

In order to have a first order phase transition there must be $N_f \geq 3$ quarks. Thus, in the case of the quark gluon-plasma, there are N_f quarks and 8 massless gluons. So we have

$$g_{QGP} = \frac{7}{8}(\underbrace{N_f \times 3 \times 2 \times 2}_{quarks}) + (\underbrace{8 \times 2}_{gluons}) + g_{both} = 10.5N_f + 16 + 14.25 = 10.5N_f + 30.25, \tag{17}$$

where for the quarks we take into account the three color variations, two possible spins, and the particle/antiparticle degrees of freedom, and we have counted the two possible polarizations of the gluons.

For the hadronic state we count only three pions[15] which are the only relativistic hadrons below the critical temperature. So,

$$g_h = \underbrace{3}_{pions} + g_{both} = 17.25 \tag{18}$$

One final ingredient for the ϵ's and P's is missing. The main difference between the QGP and the hadronic phases is the fact that quarks are confined in hadrons. One way to account for this is adding a negative pressure B (or *bag constant*) to the QGP pressure (P_{QGP}) that reflects the fact that hadrons are stopped from being free by an inward pressure. Then we add the same bag constant B to the energy density ϵ_{QGP} to account for the fact that we now have confined states in the hadronic phase. This is known as the MIT Bag Model [37]. Therefore,

$$\epsilon = \begin{cases} \frac{\pi^2}{30}T^4(10.5N_f + 30.25) + B, & \text{QGP.} \\ \frac{\pi^2}{30}T^4(17.25), & \text{hadron gas.} \end{cases} \tag{19}$$

[14] Antineutrinos are not taken into account because they have a right-handed chirality.

[15] With masses of 139 MeV for the charged pions π^+ and π^- [35] and 135 MeV for the neutral pion π^0 [36]

and (20)

$$P = \begin{cases} \frac{\pi^2}{90}T^4(10.5N_f + 30.25) - B, & \text{QGP.} \\ \frac{\pi^2}{90}T^4(17.25), & \text{hadron gas.} \end{cases} \tag{21}$$

Furthermore, we require that $B = \frac{\pi^2}{90}g_{QGP}\left(1 - \frac{g_h}{g_{QGP}}\right)T_c^4$, so that when the transition begins at $T = T_c$, the pressures are equal, $P_h = P_{QGP}$.

5 Nucleation Theory

To correctly model a first order QCD phase transition we need to use the theory of *relativistic-quantum nucleation* [38,39], which aims to calculate the transition probability from a *quantum field* associated with a certain phase, to another quantum field representing a different phase. In general, evaluating the relativistic-quantum expression for the transition probability is, due to its complexity, done numerically. For this reason, simpler models are used as a first approximation. For example, since the QGP can be treated as a relativistic fluid, Csernai and Kapusta calculated the *nucleation rate* (similar to the transition probability) of a phase into another, using relativistic hydrodynamics and classical nucleation theory [40].

For a given system, a first order phase transition occurs at a certain critical temperature. When a system has high levels of purity and there are no external agents, then it can be *superheated* or *supercooled*, meaning that the system achieves a higher or lower temperature than the critical one, respectively. As the temperature rises above the critical value, bubbles whose interior is filled with another phase are going to be nucleated but will fail to expand until a certain temperature is reached. At this temperature, the bubbles are nucleated with a *critical radius* which is the necessary radius for a bubble to grow instead of shrink. The main goal of classical nucleation theory is to compute the probability of nucleating a bubble with a critical radius per unit time per unit volume. Impurities in the original phase can trigger a faster appearance of bubbles, which is called an *heterogeneous nucleation*. If there are no impurities, it is called an *homogeneous nucleation*. We expect that a first order QCD phase transition would have proceeded as a homogeneous nucleation since it was the first QCD phase transition ever made and so there were no impurities.

Classically, the nucleation rate is expected to be proportional to a Boltzmann distribution-like function $e^{-\frac{\Delta F}{T}}$ ($k_B = 1$) because the nucleation rate is the probability of going from one configuration to another one in a thermodynamic system which can be studied as a canonical ensemble. This was deduced from first principles by Langer [41] and established that the nucleation rate has the form:

$$I = \frac{\Omega}{2\pi}\kappa e^{-\frac{\Delta F}{T}}, \tag{22}$$

where Ω is called the *statistical prefactor* which accounts for the available phase space as the system goes from one phase to another, κ is called the *dynamical prefactor* which accounts for the growth of the bubble and ΔF is the change of free energy of the system from going to one phase to the other.

The nucleation rate calculated by Csernai and Kapusta, which gives the probability of nucleating a bubble of the H-phase out of the QGP-phase (the H stands for hadron phase and the QGP stands for quark-gluon plasma, as usual), is:

$$I = \frac{1}{2\pi} \underbrace{2\left(\frac{\sigma}{3T}\right)^{3/2}\left(\frac{r_*}{\xi_{\rm QGP}}\right)^4}_{\Omega} \underbrace{\frac{4\sigma(\zeta_{\rm QGP}+4\eta_{\rm QGP}/3)}{(\Delta\omega)^2 r_*^3}}_{\kappa} e^{-\Delta F_*/T} = \frac{4}{\pi}\left(\frac{\sigma}{3T}\right)^{3/2} \frac{\sigma(3\zeta_{\rm QGP}+4\eta_{\rm QGP})r_*}{3(\Delta\omega)^2\xi_{\rm QGP}^4} e^{-\Delta F_*/T}, \tag{23}$$

where σ is the surface tension of the bubbles, T is the temperature, $\zeta_{\rm QGP}$ is the bulk viscosity of the QGP-phase, $\eta_{\rm QGP}$ is the shear viscosity of the QGP-phase, $\Delta\omega$ is the difference of enthalpy density ($\omega = P + \epsilon$) between the phases, which can be interpreted as the latent heat per volume, and $\xi_{\rm QGP}$ a correlation length to be defined below.

To completely evaluate (23) we need to know ΔF, $\eta_{\rm QGP}$, $\zeta_{\rm QGP}$, $\xi_{\rm QGP}$ and σ. The free energy difference ΔF will be evaluated in the next section. The two viscosities $\zeta_{\rm QGP}$ and $\eta_{\rm QGP}$ are, generally, related to the difficulty of the fluid to be compressed and deformed respectively. As shown in [42], for a QCD coupling constant α_s between 0 and 0.3, we have $\zeta \ll \eta$, which physically implies that the quark gluon-plasma is much easily deformed than compressed. According to Csernai and Kapusta [40], $\alpha_s = 0.23$ near a critical temperature of $T_c = 200\,\text{MeV}$. Thus, we can neglect $\zeta_{\rm QGP}$ in (23). The shear viscosity according to [43] and [44] has the general form $\eta_H = CT^3$ with C a constant determined by the number of dynamical quarks and the value of the coupling constant. For two dynamical quarks, $\eta_{\rm QGP} = 18T^3$ according to Kapusta [45]. Nevertheless, the final average bubble radius depends very weakly in the value of C. Thus, we will take $\eta_{\rm QGP} = 18T^3$ for all the scenarios considered in Section 7.

The surface tension of the bubbles σ has only been evaluated using Lattice QCD with no dynamical quarks in [46–48]. Nevertheless, to our knowledge there is not a value for a non-zero value of dynamical quarks. Csernai and Kapusta used the value of $\sigma = 50\,\text{Mev/fm}^2$, but different values had been considered ranging from $\sigma = 50\,\text{Mev/fm}^2$ to $\sigma = 450\,\text{Mev/fm}^2$ [49].

Finally, the correlation length $\xi_{\rm QGP}$ defined in [40] depends on the bubble thickness and is associated with the energy necessary to go from one phase to the other. According to Csernai and Kapusta, its value is 0.7 fm near the critical temperature $T_c \sim 200\,\text{MeV}$. Similar to the value of C in $\eta_{\rm QGP}$, the final average bubble radius depends very weakly with $\xi_{\rm QGP}$. Therefore, we will use $\xi_{\rm QGP} = 0.7\,\text{fm}$.

6 Nucleation of hadrons in the early Universe.

As stated in Section 5, the QCD phase transition is modeled through homogeneous nucleation theory with hadronic *spherical* bubbles forming in the QGP.

The first step in doing so is to identify an order parameter, so that we can follow the procedure described in Section 3. Recall that for a first order transition the order parameter must have a discontinuous behaviour at the critical temperature and note that the radius of a bubble is zero for $T > T_c$, but for $T < T_c$ there is a discontinuous jump from zero to a non-vanishing value. Then, since the radius of the bubble is closely related to the physics of the transition, we can identify it with the order parameter.

Now we must construct Landau's free energy functional F for a bubble in terms of its radius r, *i.e.* the energy required to create a bubble of radius r at environment temperature T. We begin by considering the surface tension σ of a bubble, defined as the ratio of the work W to the bubble's surface change ΔA due to W, *i.e.* σ is a proportionality factor such that the work W required to expand a bubble by ΔA is simply $\sigma\Delta A$. Therefore, the work required to *create* a bubble from nothing under our conditions has the contribution σS, with S the

bubble's surface area.

The interior and exterior of the bubbles correspond to different phases, so in principle there may be a difference of pressure at the surface of the bubble. This tells us that to nucleate a bubble of volume V, one must oppose the external pressure and there is a work contribution of the form $V\Delta P = V(P_{ext} - P_{int}) = V(P_q - P_h)$, where we have used that the exterior phase is the QGP (q) and the interior is the hadronic phase (h) and as such, these pressures are given by (21).

We will not consider other contributions (such as bubble collisions), so the total work required to create a bubble at T is,

$$W = \sigma S + V\left(P_q - P_h\right),$$

and therefore, for a bubble of radius r,

$$F = 4\pi r^2\sigma + \frac{4\pi}{3}r^3(P_q - P_h)\,.$$

By applying the equilibrium condition $\frac{\partial F}{\partial r} = 0$ (as discussed in Section 3) we find that the critical radius at which bubbles nucleate is given by

$$r_* = \frac{2\sigma}{P_h - P_q}, \tag{24}$$

which we recognize as Laplace's equation and has a corresponding Helmholtz free energy of the form

$$F_* = \frac{4\pi}{3}\sigma r_*^2\,. \tag{25}$$

Because $P_h(T_c) = P_q(T_c)$ it follows that r_* changes discontinuously when passing through T_c, which is consistent with this being a first order phase transition.

F_* is the thermodynamic potential that contains the information we are interested in. It will allow us to study how the hadronic and QGP volumes compare and evolve by considering the fraction

$$h(t) = \frac{V_h(t)}{\Omega(t)},$$

where $V_h(t)$ is the volume occupied by the hadron phase and $\Omega(t)$ is the total volume. From now on, we shall work on the comoving frame so that Ω is constant.

Recall that we are looking for a length $\bar{\ell}$ that characterizes the distance between nucleation centers at the end of the transition (Section 1). As we are about to see, $h(t)$ relates to the *radius of an average size bubble* (size meaning volume)

$$\tilde{r}(t) := \left(\frac{3}{4\pi}\bar{V}(t)\right)^{1/3}, \tag{26}$$

with $\bar{V}(t)$ the mean volume of a bubble.

First we note that at time t, the bubbles of the system may have different size, but to visualize it we can equivalently think of the system as having $N(t)$ bubbles of average size. So from Figure 4 we see that the distance between nucleation centers may be considered as $\ell = 2\tilde{r}$. As this holds for any average size bubble, then the mean of ℓ, $\bar{\ell}$, is of order $\tilde{r}$, i.e.

$$\bar{\ell} \sim \tilde{r}.$$

This order relation also accounts for the fact that in our cartoon of Figure 4 the average size spheres may not fill Ω properly.

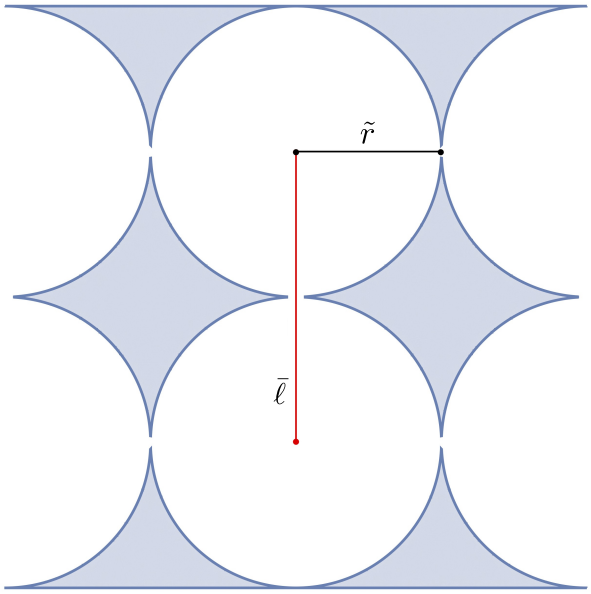

Figure 4: Cartoon of the phase transition if all bubbles were of average size $\bar{V}$, corresponding to a radius $\tilde{r}$. The QGP takes up the shaded region and the blank spaces are the hadronic bubbles. We can appreciate that the distance between nucleation centers of average size bubbles is $\ell = 2\tilde{r}$.

Therefore, knowing $\tilde{r}(t)$ satisfies our interests. Let us now relate it to $h(t)$. We need only to manipulate equation (26) in its equivalent form expressing $\bar{V}(t)$ as the arithmetic mean of the volume of the bubbles, so

$$\tilde{r}(t) \;=\; \left(\frac{3}{4\pi}\frac{\sum_{i=1}^{N(t)} V_i(t)}{N(t)}\right)^{1/3} \;=\; \left(\frac{3}{4\pi}\frac{V_h(t)}{N(t)}\right)^{1/3} \;=\; \left(\frac{3}{4\pi}\frac{V_h(t)/\Omega}{N(t)/\Omega}\right)^{1/3}. \tag{27}$$

Thus,

$$\tilde{r}(t) \;=\; \left(\frac{3}{4\pi}\frac{h(t)}{N(t)/\Omega}\right)^{1/3}. \tag{28}$$

Note that $N(t)/\Omega$ is simply the number density of bubbles, $n(t)$. This may not be obvious at first, as one may be tempted to consider only the hadronic volume, so that $n(t)$ would be $N(t)/V_h(t)$. However, the latter definition is ill. The information that interests us from a number density is the average number of bubbles in a given arbitrary subregion of the system under study (see Figure 5), obtained by multiplying the density by the volume of the subregion, and this can only be such if $n(t) = N(t)/\Omega$. For example if we consider the whole region, $n(t)\Omega = N(t)$ as it should.

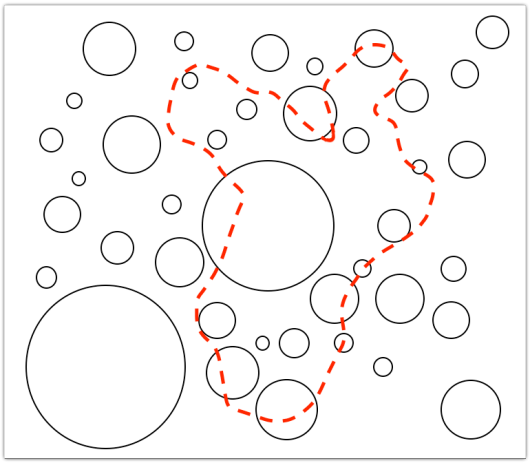

Figure 5: Cartoon of the phase transition. The number density must be obtained using the total volume Ω, as this allows us to know the average number of bubbles on an arbitrary sub-region (red).

Therefore $N(t)/\Omega$ is indeed the bubble number density and we have found that

$$\tilde{r}(t) = \left(\frac{3}{4\pi}\frac{h(t)}{n(t)}\right)^{1/3}. \tag{29}$$

We shall now derive an expression for the hadronic volume $V_h(t)$ that will automatically provide us with one for $h(t)$ itself. Because the critical radius of a bubble depends on the difference of the phase pressures, as seen in (24), then the critical radius depends on time (through temperature). Thus, the size of a bubble depends on the time of creation t' and the coordinate time t, which accounts for the growing of the bubble. So, we have a function of the form $V(t,t')$ that considers the initial volume $V(t',t')$ and the expansion from t' to t.

In order to compute the hadronic volume $V_h(t)$, we need to add the contributions of each bubble with size $V(t,t')$. Therefore, we need the number of bubbles nucleated. This is where the nucleation rate comes into play, because it quantifies how many bubbles are successfully nucleated per unit time per unit volume, which implies that the number of bubbles of critical sized formed in a time dt' in the available space $V_q(t')$[16] is $dt'I(t')V_q(t')$. Using that the QGP volume is $V_q = (1-h(t'))\Omega$ and adding the contributions of all the bubbles nucleated we get that the hadronic volume is

$$h(t)\Omega := V_h(t) = \int_{t_c}^{t} dt' I(t') V_q(t') V(t,t') = \int_{t_c}^{t} dt' I(t')(1-h(t'))\Omega V(t,t'), \tag{30}$$

where t_c is the critical time at which the transition occurs. Since Ω is constant, we have

$$h(t) \;=\; \int_{t_c}^{t} dt' I(t')(1-h(t'))V(t,t'). \tag{31}$$

Eq. (31) is an integral equation for $h(t)$ that, when coupled to the cosmological evolution of the Universe, provides the aspects of the QCD phase transition that we are interested in. However, before doing the coupling, we need an explicit expression for $V(t,t')$, which can be obtained by rewriting V as

$$V(t,t') = \frac{4}{3}\pi(r(t') + \Delta r(t,t'))^3 = \frac{4}{3}\pi\left(r_*(t') + \Delta r(t,t')\right)^3,$$

[16]The available space is $V_q(t')$ because bubbles cannot be created in the space that has already been transformed to the hadronic phase.

so that $\Delta r(t,t')$ accounts for the expansion of the bubble; we are no taking into account the growth of the bubbles due to the expansion of the Universe because, as we said earlier, we are working in the comoving frame. Therefore, if $v(t'')$ is the speed of the expanding surface of the bubble, then $\Delta r\left(t'\right) = \int_{t'}^{t} dt'' v(t'')$. Thus,

$$V(t,t') = \frac{4}{3}\pi\left(r_*\left(t'\right) + \int_{t'}^{t} dt'' v\left(t''\right)\right)^3 \tag{32}$$

Furthermore, the bubble interface speed growth $v(T)$ was computed numerically by Miller and Pantano [50]. The computation was made using relativistic hydrodynamics with the equations of state given by (19). Thus, one expects that the dependence of the speed with time is realized through the temperature. Then, the speed is given by

$$v(T(t)) = 3\left(1 - \frac{T(t)}{T_c}\right)^{3/2}. \tag{33}$$

To compute $\tilde{r}$ with equation (29), we must also know the expression for $n(t)$, or equivalently $N(t)$.

As previously discussed, the number of bubbles produced in a time dt' is $dt' I(t')(1-h(t'))\Omega$. Thus

$$N(t) = \int_{t_c}^{t} dt' I(t')(1 - h(t'))\Omega$$

and therefore

$$n(t) = \int_{t_c}^{t} dt' I(t')(1 - h(t')). \tag{34}$$

Hitherto we have not coupled T with time nor our system with the dynamics of space-time, this can be achieved by using equations (5a) and (7). First we note that equation (7) implies that

$$\frac{d\epsilon}{da} = -\frac{3\omega}{a}\,. \tag{35}$$

Note that unlike the $\Delta\omega$ on (23), ω is the enthalpy density of the hole system and the analogous is true for ϵ. Given the extensive nature of energy and enthalpy, they must be given by the sum of their parts (hadrons and QGP) weighted by their respective volume fraction, so their densities satisfy,

$$\begin{aligned} \epsilon(t) &= h(t)\epsilon_h(t) + (1 - h(t))\epsilon_q(t) \\ \omega(t) &= h(t)\omega_h(t) + (1 - h(t))\omega_q(t). \end{aligned} \tag{36}$$

Equation (35) couples our model to a through (11). However, due to the time integration on (31) it is still necessary to relate a with t. This is precisely what eq. (5a) does.

As discussed in section 2, the k on equation (5a) relates to the curvature of space. Because this transition happened after inflation, we can consider k to be zero and therefore equation (5a) reduces to:

$$\frac{\dot{a}}{a} = \sqrt{\frac{8\pi}{3}\epsilon}\,. \tag{37}$$

Eqs. (31) and (35) define a system of integro-differential equations that determine the cosmological evolution of the phase transition where the dependant variables are the scale factor h and T which depend on the scale factor $a(t)$. After solving for h and T we can compute the bubble number density through (34) and the radius of an average size bubble with (29). We will now proceed to arrange the equations in a numerical-friendly way.

First, we have to rewrite equation (31) in terms of the scale factor $a(t)$. Using equation (37) to get the Jacobian, then

$$h(a) = \int_{a_c}^{a} da' \frac{1}{a'} \sqrt{\frac{3}{8\pi G \epsilon(a')}}\, I(T(a'))(1 - h(a'))V(a, a'), \tag{38}$$

where the nucleation rate is given by equation (23) and the volume $V(t, t')$ given by equation (32). The nucleation rate depends on the values $\sigma = 50, 150, 200\,\mathrm{MeV/fm^2}$, $\eta = 18T^3$, $\zeta = 0$, $\xi = 0.7\,\mathrm{fm}$, the critical radius given by equation (24), the equilibrium Helmholtz free energy given by (25), and the enthalpy difference $\Delta\omega = \omega_q - \omega_h$. The enthalpies given by $\omega_i = \epsilon_i + P_i$, for $i = q, h$, can be calculated through equations in (19).

For equation (37), we must solve for $\frac{dT}{da}$. For this we plug equations (11) with (19) into equation (37), which gives

$$\frac{dT}{da} = -\frac{\dfrac{3w(a)}{a} + \dfrac{dh}{da}\left[\epsilon_h(T(a)) + \epsilon_q(T(a))\right]}{h(a)\dfrac{d\epsilon_h}{dT} + (1 - h(a))\dfrac{d\epsilon_q}{dT}}. \tag{39}$$

Thus, the system of equations to solve are (38) and (39).

A complete discussion of how to solve these equations can be found in `https://github.com/davidguzmanr/QCD-phase-transitions`.

7 Results

In Fig. 6 we plot the evolution of the temperature, the nucleation rate, the bubble density, the radius of an average size bubble, the energy and enthalpy densities, and the hadron fraction, with respect to the scale factor (which, in turn, is related to time through Friedmann equations) for different values for the surface tension, namely $\sigma = 50$, 150 and 200 $\mathrm{MeV/fm^2}$. As discussed before, the value of σ for a non-zero value of dynamical quarks is not already known. So, we choose a set of values used in previous works.

We can see in Fig. 6(a) an identical behaviour like in [45]. The first part consists in a decrease in temperature due to the cosmic expansion. The temperature arrives at values lesser than the critical temperature, indicating the presence of a supercooling effect. Afterwards, there is a rise in temperature (known as reheating) due to the release of latent heat during the formation of bubbles, as can be seen comparing Fig. 6(a) with Fig. 6(f) and Fig. 6(b). The enthalpy in Figure 6(f) is negative by convention. At first, it increases reaching a maximum and then having an abrupt decrease meaning this latent heat has been released. The release of latent heat comes from the energy lost by the quarks as they confine and indicates that this phase transition is exothermic. After that, the temperature increases less rapidly. Before explaining what happens during this stage of lesser increase in the temperature, we can further clarify the nucleation of bubbles. In Fig. 6(c) we see the effective appearance of bubbles of critical size radius and in Fig. 6(d) we can see a discontinuous growth of the radius, both occurring during

the reheating. In Figure 6(d) the discontinuous jump during reheating is characteristic of a first order phase transition. This jump is also observed in Figure 6(c) where the number density jumps from zero to a finite value meaning that all bubbles are nucleated during the reheating. Then, the same number of bubbles nucleated begin to grow during the phase of lesser increase in the temperature, and no more are created since the nucleation rate vanishes as seen in Figure 6(b). After the reheating, in the stage of a less rapid increase in the temperature, the nucleated bubbles begin to occupy the space, as can be seen in Fig. 6(g), until the hadron fraction is equal to one, meaning there is no QGP left in the comoving volume. Then, the transition is completed and the equations used for this analysis are no more valid.

The surface tension changes the magnitude of the nucleation rate I and the time at which it happens. A greater surface tension means that more energy is needed to nucleate a bubble. Since the initial energy density is the same for the three cases as seen in Fig. 6(e), then, lesser bubbles are going to be nucleated for a greater surface tension, and these are going to be nucleated later because it is needed a greater supercooling to overcome the energy used to create the bubbles. Despite this, there is no change in the continuous decrease of the energy density due to the cosmic expansion as seen in Fig. 6(e). The value of the surface tension does not affect the energy because it only depends on the type of fluids considered and the temperature as seen in equation (13). The behaviour observed in Figure 6(e) is consistent with being a relativistic fluid. Furthermore, we can see that for smaller radius in Fig. 6(d), the bubble number density has to be higher in order to reach $h = 1$ in the same amount of time.

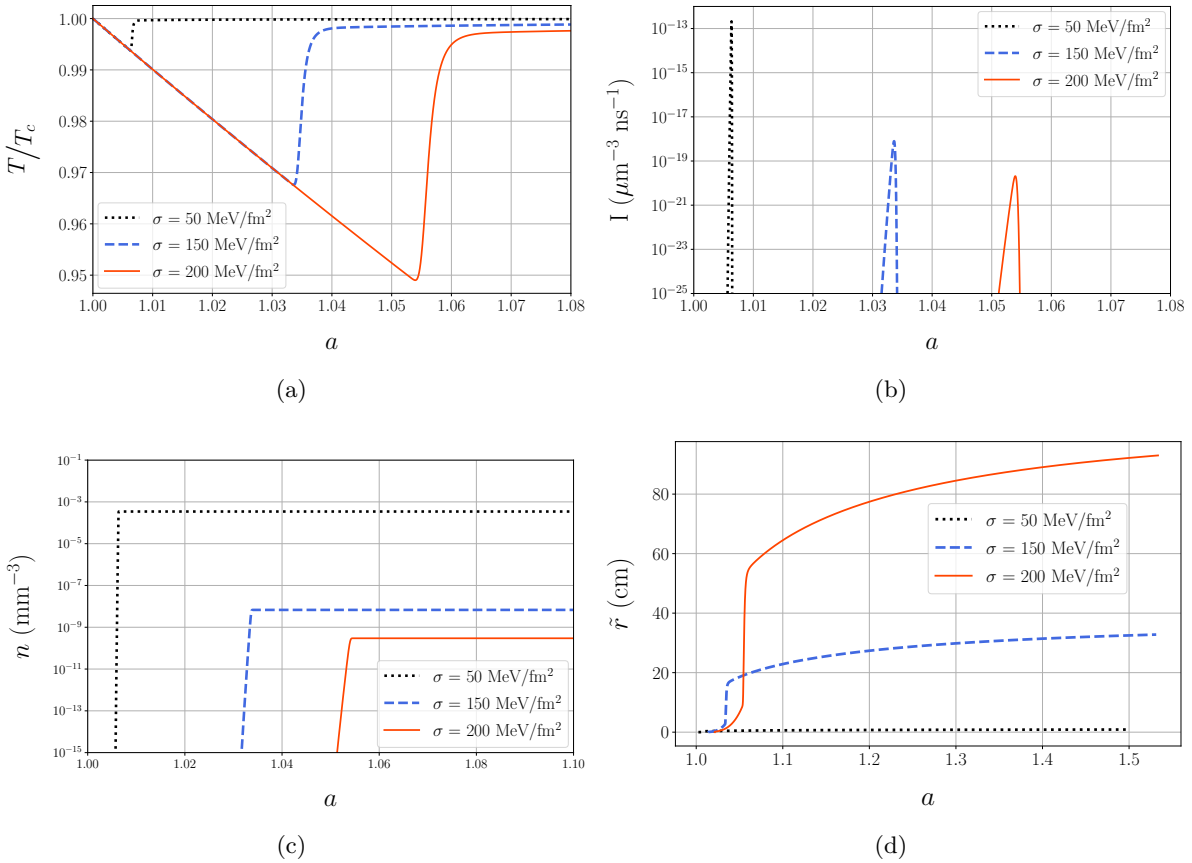

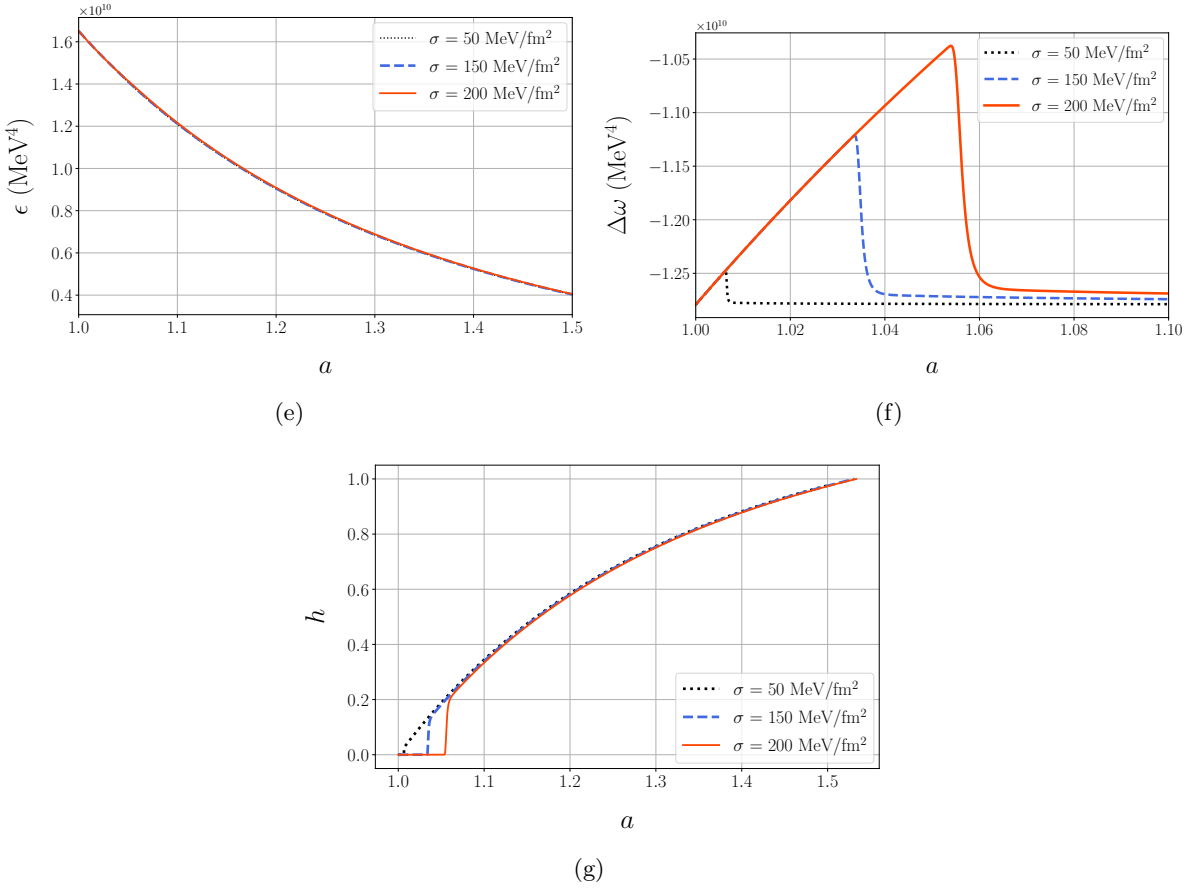

Figure 6: Evolution with respect to the scale factor a of (a) temperature T, (b) nucleation rate I, (c) bubble density n, (d) radius of an average size bubble $\bar{r}$ (the black dotted curves is non zero but much less than the other curves), (e) energy density ϵ, (f) enthalpy density or latent heat $\Delta\omega$ and (g) hadron fraction h for $\eta = 18T^3$, $\xi = 0.7\,\mathrm{fm}$, $\zeta = 0$, $g_h = 17.25$, $T_c = 160\,\mathrm{MeV}$, $g_q = 61.75$ (3 quarks) and $\sigma = 50,\ 150,\ 200\,\mathrm{MeV/fm^2}$.

As a next case, we consider the evolution of the same dynamical quantities in Fig. 7 for different values for the critical temperature, namely $T_c = 160$, 180 and 200 MeV. The plots of N, I, $\Delta\omega$ have their peaks at the same moment as in Figure 7(a) and behave similarly to Fig. 6. This means that for an earlier peak in the temperature, the nucleation rate is bigger and the number density is higher. We can see that the peak at which the bubbles start to nucleate happen before for higher critical temperatures. This is because for higher critical temperature the energy density is higher, as seen in Figure 7(c), therefore, because the surface energy is fixed the amount of energy necessary to start creating bubbles will be fulfilled before with higher energy density. From eq. (33) and Fig. 7(a) we can see that a greater critical temperature implies a lower speed of the expansion of the bubbles. This means that more bubbles are going to be nucleated in the same comoving volume because there is going to be more space without bubbles during the reheating phase (when the nucleation rate value is non-zero). The above reasoning is pictured in Fig. 7(b), where we see bubbles with a smaller radius for greater critical temperatures which implies a bigger number density. Furthermore, the bubble radius increases with lesser critical temperature but not significantly as seen in Figure 7(b) and the duration of the transition is the same for all three critical temperatures as seen in Fig. 7(d).

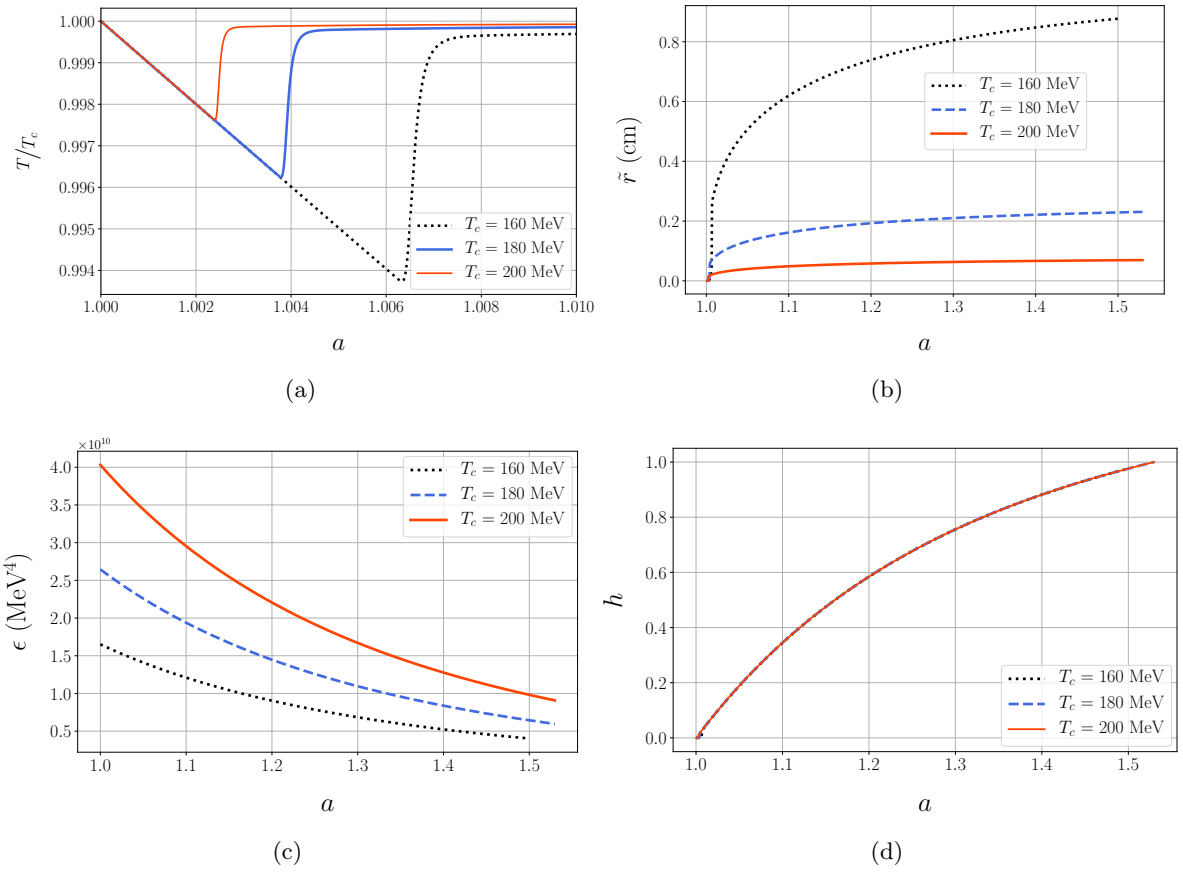

Figure 7: Evolution with respect to the scale factor a of (a) temperature T, (b) radius of an average size bubble $\bar{r}$, (c) energy density ϵ and (d) hadron fraction h for $\eta = 18T^3$, $\xi = 0.7\,\text{fm}$, $\zeta = 0$, $\sigma = 50\,\text{MeV/fm}^2$, $g_h = 17.25$, $g_q = 61.75$ (3 quarks) and $T_c = 160,\ 180,\ 200\,\text{MeV}$.

Finally, we studied the evolution bubbles for a different number of quarks and we plot the results in Fig. 8. From equation (13) we see that the energy density must be higher with more quarks. This is depicted in Fig. 8(c), but in all cases the energy density decreases which is consistent with the whole fluid being relativistic matter. Because for higher number of quark the energy density is higher, then the creation of bubbles happens before as seen in the peak of Fig. 8(a). The bubble radius changes but not significantly as seen in Fig. 8(b). Nevertheless, there is a change in the duration of the transition as seen in Fig. 8(d).

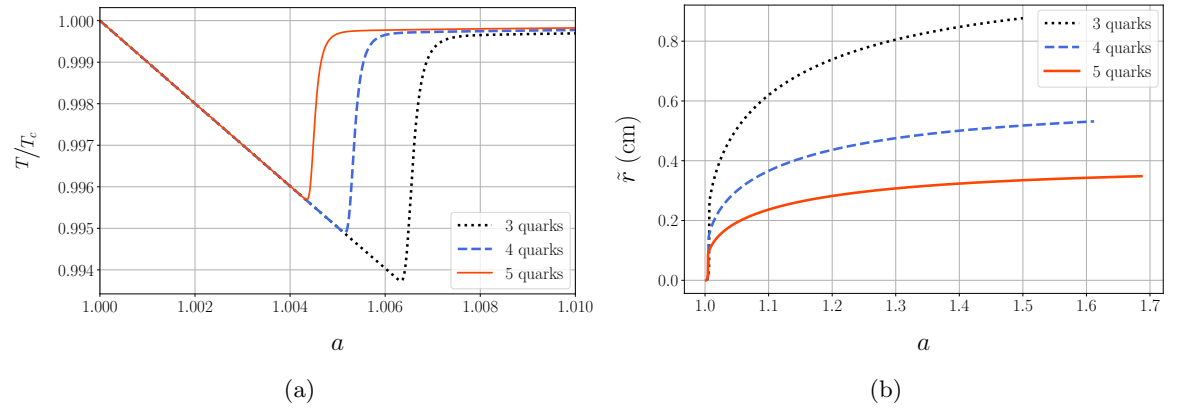

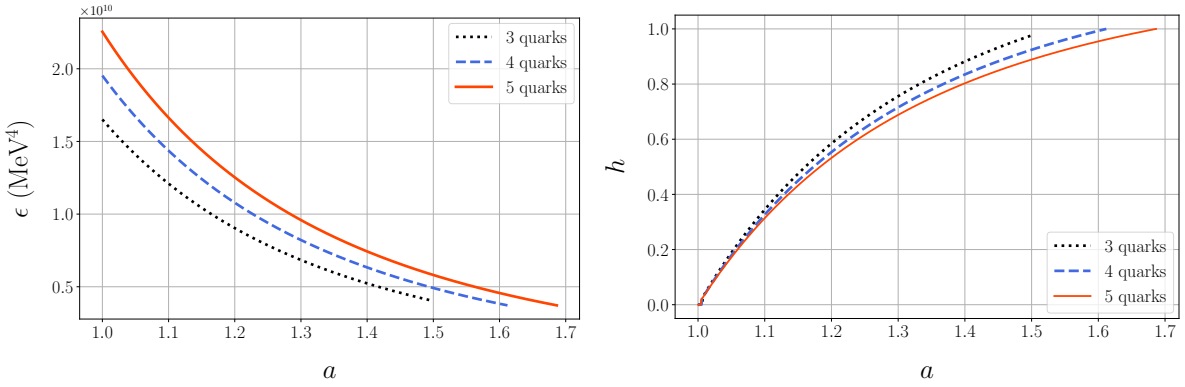

(c) (d)

Figure 8: Evolution with respect to the scale factor a of (a) temperature T, (b) Radius of an average size bubble $\tilde{r}$, (c) energy density ϵ and (d) hadron fraction h for $\eta = 18T^3$, $\xi = 0.7\,\text{fm}$, $\zeta = 0$, $g_h = 17.25$, $T_c = 160\,\text{MeV}$, $\sigma = 50\,\text{MeV/fm}^2$ and $N_f = 3, 4, 5$ quarks.

8 Final remarks and outlook

We have introduced basic concepts in order to understand the evolution of a cosmological QCD confinement first order phase transition using the MIT bag model. In Section 2 we introduced some basic concepts of standard cosmology. In Section 3 we reviewed basic aspects of phase transitions emphasizing in first order phase transitions and explain the concept of crossover. In Section 4, we explained the conjectured QCD Phase diagram and mention the conditions in which the phase transition proceeded as first order and the equation of state of the QGP and the hadron gas in the MIT bag model. In Section 5 we introduced basic concepts of nucleation theory and gave an intuitive idea of the nucleation rate of hadronic bubbles in a QGP. Then, in section 6 we finally used the concepts previously introduced in order to establish the set of integro-differential equations which must be solved numerically. Finally, in Section 7 we discussed and analyzed the behaviour of the transition varying the surface tension $\sigma = 50, 150, 200\,\text{MeV}$, the critical temperature $T_c = 160, 180, 200\,\text{MeV}$ and the number of dynamical quarks $N_f = 3, 4, 5$ quarks.

The general description of the evolution of the bubbles during the QCD first order phase transition is as follows: the cosmic expansion causes a decrease in the temperature of the Universe and reduces the interaction between the existent particles. The QGP does not transforms to the hadron gas at the critical temperature because of the purity of the universe. The QGP supercools below the critical temperature, because it needs energy to overcome the expense of forming the surface of the hadron bubbles. At a certain point, the probability to nucleate a bubble begins to grow. The nucleation of bubbles releases latent heat to the thermal bath, thus reheating the Universe until the temperature is near its critical value; the energy released by the bubbles comes from the energy lost by the quarks as they are confined into hadrons. After that, both phases coexist at the same pressure and the hadronic bubbles continue their grow, releasing enough energy to increase the temperature. The transition ends when all the QGP has been converted into hadrons. Later, the cosmic expansion will decrease the temperature, continuing the thermal history of the Universe.

The contents of this article will hopefully be useful for a graduate or advanced undergraduate student who is pursuing starting to study a cosmological QCD phase transition. As stated in the introduction, the applications of a QCD first order phase transition include the influence

on nucleosynthesis and the production of gravitational waves. Furthermore, the model can be extended adding a chemical potential as in [51]. This article may be the starting point in a project involving one of these.

Acknowledgments. It is a pleasure to thank Alejandro Ayala, Víctor Romero-Rochín, Eugenio Ley-Koo... for insightful discussions. This work was partly supported by DGAPA-PAPIIT grant IN100217 and CONACyT grants F-252167 and 278017. The work of S.R-S. is supported by the Deutsche Forschungsgemeinschaft (SFB1258) and the TUM AugustWilhelm Scheer Program.

A Curvature in three spatial dimensions

From the Friedmann-Lemaître-Robertson-Walker interval (3),

$$ds^2 = \sum_{\mu=0}^{3}\sum_{\nu=0}^{3} g_{\mu\nu}\, dx^\mu dx^\nu = dt^2 - a(t)^2 \left(\frac{dr^2}{1-k\,r^2} + r^2\, d\vartheta^2 + r^2 \sin^2\vartheta\, d\varphi^2 \right) ,$$

we see that the three-dimensional space (ignoring time) is characterized by the interval

$$d\tilde{s}^2 = \sum_{i=1}^{3}\sum_{j=1}^{3} g_{ij}\, dx^i dx^j = \frac{dr^2}{1-k\,r^2} + r^2\, d\vartheta^2 + r^2 \sin^2\vartheta\, d\varphi^2 , \qquad i,j = 1,2,3 , \tag{40}$$

where $x^1 = r$, $x^2 = \vartheta$ and $x^3 = \varphi$ are the usual spherical coordinates, and k is a real constant. The same information is contained in the metric tensor g, which in this case can be represented by the 3×3 diagonal matrix representation

$$g = (g_{ij}) = \begin{pmatrix} (1-kr^2)^{-1} & 0 & 0 \\ 0 & r^2 & 0 \\ 0 & 0 & r^2 \sin^2\vartheta \end{pmatrix} . \tag{41}$$

The inverse g^{-1} of the metric tensor is represented by the diagonal matrix (note the position of the indices)

$$g^{-1} = (g^{ij}) = \begin{pmatrix} 1-kr^2 & 0 & 0 \\ 0 & r^{-2} & 0 \\ 0 & 0 & r^{-2}\csc^2\vartheta \end{pmatrix} . \tag{42}$$

In order to describe the curvature properties of this space, it is useful to define the so-called *Christoffel symbols*,

$$\Gamma^i{}_{j\ell} = \frac{1}{2}\sum_{m=1}^{3} g^{im} \left(\frac{\partial g_{mj}}{\partial x^\ell} + \frac{\partial g_{\ell m}}{\partial x^j} - \frac{\partial g_{j\ell}}{\partial x^m} \right) , \qquad i,j,\ell = 1,\ldots,3 , \tag{43}$$

which help one express the *Riemann curvature tensor*, whose 3^4 components,

$$R^\ell{}_{imj} = \frac{\partial}{\partial x^m}\Gamma^\ell{}_{ij} - \sum_{n=1}^{3} \Gamma^\ell{}_{nj}\Gamma^n{}_{im} - \frac{\partial}{\partial x^j}\Gamma^\ell{}_{im} + \sum_{n=1}^{3} \Gamma^\ell{}_{nm}\Gamma^n{}_{ij} , \qquad i,j,\ell,m = 1,\ldots,3 , \tag{44}$$

contain all information on how a three-dimensional space endowed with a metric g deviates from flatness. The space is curved only if some of these components are non-zero. From the

Riemann tensor, it is possible to derive two important quantities, the *Ricci tensor* and the *Ricci scalar*,

$$R_{ij} = \sum_{\ell=1}^{3} R^{\ell}{}_{i\ell j} \qquad \text{and} \qquad R = \sum_{i=1}^{3}\sum_{j=1}^{3} g^{ij} R_{ij}\,, \tag{45}$$

respectively.

Applying the previous definitions with the metric tensor g encoded in (40), one can show that the non-vanishing components of the Riemann tensor are

$$\begin{aligned} R^{2}{}_{121} &= R^{3}{}_{131} = -R^{2}{}_{112} = -R^{3}{}_{113} = k/(1-k\,r^2)\,, \\ R^{1}{}_{212} &= R^{3}{}_{232} = -R^{1}{}_{221} = -R^{3}{}_{223} = k\,r^2\,, \\ R^{1}{}_{313} &= R^{2}{}_{323} = -R^{1}{}_{331} = -R^{2}{}_{332} = k\,r^2\,\sin^2\vartheta\,. \end{aligned} \tag{46}$$

Further, the Ricci tensor components are given by $R_{ij} = 2k g_{ij}$ and, consequently, the Ricci scalar reads $R = 6k$. This means that k is a scalar measurement of the curvature. Note that $k = 0$ yields $R^{\ell}{}_{imj} = R_{ij} = R = 0$, i.e. it corresponds to a flat (Euclidean) three-dimensional space.

B Glossary

Since many new concepts are used in this work, we provide here a concise description of some of them to help a reader who is getting acquainted with this research area. We consider that the concepts listed below are fundamental to follow our discussion and are not directly accessible in a first search in the existing literature. The brief definitions provided here do not replace a careful study of the corresponding topics, which are also discussed in greater depth in the main text.

- **Baryon density contrast.** It is an inhomogeneity appearing in growing hadronic bubbles within a quark-gluon plasma (QGP). This inhomogeneity emerges because quark states, contributing to the baryon density, are energetically favored in the QGP rather than in the hadronic phase. This is a consequence of the chiral symmetry breakdown, which greatly enhances the effective mass of quarks in hadrons.
- **Shear and bulk viscosity.** Shear viscosity measures the resistance of a fluid to be deformed by a shear stress, while bulk viscosity measures its resistance to a shearless compression.
- **Chiral transition.** It is the transition that happens in QCD when the chiral symmetry is spontaneously broken (which is the origin of hadron masses).
- **Correlation length.** It is the typical distance at which a quantity in a system starts to be uncorrelated. In this work, ξ_{QGP} represents the correlation length for the energy density of the QGP as a function of the distance from the center of a growing hadronic bubble in the QGP media while quarks and gluons hadronize during the QCD phase transition, assuming that it is first order.
- **Crossover.** It is a transition in a thermodynamic system where the divergences and discontinuities of the free energy function, characteristic of real phase transitions, are replaced by maxima and inflection points. The temperature at which this happens along with a width related to the curvature of the maxima defines a temperature band that, when crossed, induces a change of state in the system.

- **Deconfinement-confinement transition.** Also known as quark-hadron or QCD phase transition, it is the transition that happens in QCD between its two phases: free quark states at high temperatures, and groups of quarks confined in nuclear distances building up hadrons at lower temperatures. This work is devoted to the study of the dynamics during this transition.

- **Inhomogeneous big bang nucleosynthesis (BBN).** It is the generation of light nuclei in the early universe, where the abundances of the light nuclei depend on the inhomogeneities in the matter content of the Universe encoded in the baryon density contrast and the proton-to-neutron ratio density contrast.

- **MIT bag model.** It is one of the simplest semi-classical approximations introduced to understand the large-distance behavior of QCD. It considers both the hadron and QGP states as relativistic perfect fluids confined to a finite region of space (the *bag*) by an inward additional pressure, or bag constant, B, added to the potential energy of the QCD Lagrangian.

- **Supercooling and superreheating.** It is the cooling (heating) of a thermodynamic system beyond its critical temperature without letting the system go through a phase transition. At a certain temperature, which depends on the system, after the critical temperature, the system starts to create bubbles or droplets of the low (high) temperature phase and the temperature starts to increase (decrease) in what is known as thermal reheating (cooling).

References

[1] A. D. Sakharov, Pisma Zh. Eksp. Teor. Fiz. **5** (1967), 32, [Usp. Fiz. Nauk161,no.5,61(1991)].

[2] D. J. Gross and F. Wilczek, Phys. Rev. Lett. **30** (1973), 1343, [,271(1973)].

[3] H. D. Politzer, Phys. Rev. Lett. **30** (1973), 1346, [,274(1973)].

[4] T. Bhattacharya et al., Phys. Rev. Lett. **113** (2014), no. 8, 082001, `arXiv:1402.5175` [hep-lat].

[5] E. Laermann and O. Philipsen, Ann. Rev. Nucl. Part. Sci. **53** (2003), 163, `arXiv:hep-ph/0303042` [hep-ph].

[6] M. D'Elia, Nucl. Phys. **A982** (2019), 99, `arXiv:1809.10660` [hep-lat].

[7] H. Kurki-Suonio, Space Sci. Rev. **100** (2002), 249, `arXiv:astro-ph/0112182` [astro-ph].

[8] J. I. Kapusta and K. A. Olive, Phys. Lett. **B209** (1988), 295.

[9] D. J. Schwarz, Annalen Phys. **12** (2003), 220, `arXiv:astro-ph/0303574` [astro-ph].

[10] LIGO Scientific, Virgo, B. P. Abbott et al., Phys. Rev. Lett. **116** (2016), no. 6, 061102, `arXiv:1602.03837` [gr-qc].

[11] C. Caprini, *Gravitational waves from cosmological phase transitions*, in *Proceedings, 45th Rencontres de Moriond on Cosmology: La Thuile, Italy, March 13-20, 2010*, 2010, pp. 257–264.

[12] Y. Aoki, G. Endrodi, Z. Fodor, S. D. Katz, and K. K. Szabo, Nature **443** (2006), 675, arXiv:hep-lat/0611014 [hep-lat].

[13] H. Davoudiasl, Phys. Rev. Lett. **123** (2019), no. 10, 101102, arXiv:1902.07805 [hep-ph].

[14] D. Croon, J. N. Howard, S. Ipek, and T. M. P. Tait, *QCD Baryogenesis*, 2019.

[15] S. Schettler, T. Boeckel, and J. Schaffner-Bielich, Phys. Rev. **D83** (2011), 064030, arXiv:1010.4857 [astro-ph.CO].

[16] S. M. Carroll, arXiv:gr-qc/9712019 [gr-qc].

[17] B. F. Schutz, *A first course in general relativity*, Cambridge Univ. Pr., Cambridge, UK, 1985.

[18] S. Weinberg, *Gravitation and Cosmology*, John Wiley and Sons, New York, 1972.

[19] Planck, N. Aghanim et al., arXiv:1807.06209 [astro-ph.CO].

[20] D. Baumann, *Cosmology*, Lecture notes, 2019.

[21] P. Chaddah, *First order phase transitions of magnetic materials: Broad and interrupted transitions*, CRC Press, 2017.

[22] H. J. Cleaves, Supercritical Fluid, 1, Springer Berlin Heidelberg, Berlin, Heidelberg, 2014, pp. 1–1.

[23] G. Simeoni, T. Bryk, F. Gorelli, M. Krisch, G. Ruocco, M. Santoro, and T. Scopigno, Nature Physics **6** (2010), 503.

[24] D. Banuti, M. Raju, and M. Ihme, Supercritical pseudoboiling for general fluids and its application to injection, 211, 01 2016, pp. 211–221.

[25] Y. Aoki, Z. Fodor, S. D. Katz, and K. K. Szabo, Phys. Lett. **B643** (2006), 46, arXiv:hep-lat/0609068 [hep-lat].

[26] F. Maxim, C. Contescu, P. Boillat, B. Niceno, K. Karalis, A. Testino, and C. Ludwig, Nature Communications **10** (2019), 1.

[27] P. Linstrom, *Nist chemistry webbook, nist standard reference database 69*, 1997.

[28] H. Sazdjian, EPJ Web Conf. **137** (2017), 02001, arXiv:1612.04078 [hep-ph].

[29] K. Fukushima and T. Hatsuda, Rept. Prog. Phys. **74** (2011), 014001, arXiv:1005.4814 [hep-ph].

[30] A. Ayala, J. Phys. Conf. Ser. **761** (2016), no. 1, 012066, arXiv:1608.04378 [hep-ph].

[31] A. Bender, G. I. Poulis, C. D. Roberts, S. M. Schmidt, and A. W. Thomas, Phys. Lett. **B431** (1998), 263, arXiv:nucl-th/9710069 [nucl-th].

[32] M. A. Stephanov, PoS **LAT2006** (2006), 024, arXiv:hep-lat/0701002 [hep-lat].

[33] R. D. Pisarski and F. Wilczek, Phys. Rev. **D29** (1984), 338.

[34] ALEPH, DELPHI, L3, OPAL, SLD, LEP Electroweak Working Group, SLD Electroweak Group, SLD Heavy Flavour Group, S. Schael et al., Phys. Rept. **427** (2006), 257, arXiv:hep-ex/0509008 [hep-ex].

[35] M. Trassinelli et al., Phys. Lett. **B759** (2016), 583, arXiv:1605.03300 [physics.atom-ph].

[36] J. F. Crawford, M. Daum, R. Frosch, B. Jost, P. R. Kettle, R. M. Marshall, B. K. Wright, and K. O. H. Ziock, Phys. Rev. **D43** (1991), 46.

[37] A. Chodos, R. L. Jaffe, K. Johnson, C. B. Thorn, and V. F. Weisskopf, Phys. Rev. **D9** (1974), 3471.

[38] I. Affleck, Phys. Rev. Lett. **46** (1981), 388.

[39] A. D. Linde, Nucl. Phys. **B216** (1983), 421, [Erratum: Nucl. Phys.B223,544(1983)].

[40] L. P. Csernai and J. I. Kapusta, Phys. Rev. **D46** (1992), 1379.

[41] J. S. Langer, Annals Phys. **54** (1969), 258.

[42] P. B. Arnold, C. Dogan, and G. D. Moore, Phys. Rev. **D74** (2006), 085021, arXiv:hep-ph/0608012 [hep-ph].

[43] G. Baym, H. Monien, C. J. Pethick, and D. G. Ravenhall, Phys. Rev. Lett. **64** (1990), 1867.

[44] P. B. Arnold, G. D. Moore, and L. G. Yaffe, JHEP **05** (2003), 051, arXiv:hep-ph/0302165 [hep-ph].

[45] J. I. Kapusta and C. Gale, *Finite-temperature field theory: Principles and applications*, Cambridge Monographs on Mathematical Physics, Cambridge University Press, 2011.

[46] K. Kajantie, L. Karkkainen, and K. Rummukainen, Nucl. Phys. **B333** (1990), 100.

[47] B. Beinlich, F. Karsch, and A. Peikert, Phys. Lett. **B390** (1997), 268, arXiv:hep-lat/9608141 [hep-lat].

[48] S. Huang, J. Potvin, C. Rebbi, and S. Sanielevici, Phys. Rev. **D42** (1990), 2864, [Erratum: Phys. Rev.D43,2056(1991)].

[49] T. Boeckel and J. Schaffner-Bielich, Phys. Rev. **D85** (2012), 103506, arXiv:1105.0832 [astro-ph.CO].

[50] J. C. Miller and O. Pantano, Phys. Rev. **D42** (1990), 3334.

[51] J. I. Kapusta, A. P. Vischer, and R. Venugopalan, Phys. Rev. **C51** (1995), 901, arXiv:nucl-th/9408029 [nucl-th].